

ON THE STATIC AND CREEP STRENGTH OF MA957 FROM ROOM TEMPERATURE TO 1000°C -
 M.C. Salston and G.R. Odette (*Department of Mechanical Engineering, University of California, Santa Barbara*)

OBJECTIVE

The objective of this work is to characterize the constitutive properties of MA957 and to analyze this data to assess the factors that control the tensile and creep strength of nanostructured ferritic alloys (NFA).

SUMMARY

Static tensile and creep tests were carried out on as-extruded (AE) MA957 from room temperature to 1000°C. Comparison of these results to data taken from the literature show the yield stress (σ_y) and ultimate tensile strength of MA957 are generally higher than for 9 Cr tempered martensitic steels (TMS), like Eurofer97. However, the static tensile strength of MA957 varies by up to a factor of 2, or more, depending on the post extrusion thermal mechanical heat treatment (TMT) and specimen orientation with respect to the extrusion direction. The corresponding creep strength varies by up to a factor of ≈ 10 . The AE and TMT variants of MA957 were fit to a threshold stress (σ_{tr}) model. The $\sigma_{tr}(T)$ for the AE MA957 is $\geq 0.4\sigma_y(T)$ up to 800°C and decreases at higher temperatures, approaching 0 at 1000°C.

PROGRESS AND STATUS

Introduction

Nano-structured ferritic alloys (NFA) offer great promise for advanced fission and fusion reactors. NFA are ferritic stainless steels that contain 12-14 Cr and are dispersion strengthened by a high density of nm-scale Y-Ti-O nanofeatures (NF) that result in remarkable high temperature creep strength and radiation damage resistance [1]. NFA are processed by mechanically alloying metal powders with Y_2O_3 by ball milling, followed by hot consolidation, usually by extrusion. Our objective is to characterize and model the constitutive properties of a commercial vendor NFA INCO MA957 in the as-extruded condition, and to compare this material to other NFA and MA957 conditions, as well as to a 9 Cr tempered martensitic steel (TMS) Eurofer97.

Experimental Procedures

The composition of MA957 is 14Cr-1Ti-0.3Mo-0.22Y₂O₃(wt.%). Tensile specimens (gauge dimensions 0.5x1.2 x 5 mm) were tested in air in the axial extrusion orientation on a MTS load frame at a strain rate ($\dot{\epsilon}$) of $1.33 \times 10^{-3} \text{ s}^{-1}$ in a furnace from ambient temperature to 1000°C. Corresponding strain-rate jump (SRJ) creep tests were carried from 600 to 1000°C, starting at a relatively low imposed $\dot{\epsilon}$, usually 10^{-7} s^{-1} , until a constant steady-state stress (σ) level was reached. The $\dot{\epsilon}$ was then changed, typically increasing by an order of magnitude, and held until a new steady-state σ was reached. A sequence of such SRJ were used to characterize $\sigma(T, \dot{\epsilon})$. Creep tests were also carried out under constant load, and subsequently, under constant stress to rupture conditions.

Results

Tensile test data for several conditions of MA957 and TMS Eurofer97 [2,3,4] plotted in Figure 1a show: a) a wide range of σ_y in MA957, that vary by factors up to more than 2, depending on the alloy condition; and that b) MA957 is generally much stronger than Eurofer97. Figure 1b summarizes the corresponding creep strength for various MA957 conditions in a Larson-Miller Plot (LMP) for the creep rupture time ($C = 30$), along with data for Eurofer97 and NFA JYWT [3,4,5,6]. The various MA957 conditions and JYWT also show a wide range of creep strengths, up to a factor of ≈ 10 . The NFA creep strengths are also generally much higher than for Eurofer97. However, the open cross symbols show the hoop strength biaxial creep tests of extruded tubing is much lower than for the other NFA, and is comparable to that for Eurofer97. Figure 2 shows a Larson-Miller plot for the inverse minimum creep rate for the AE MA957 data

as well as a data set reported by Wilshire et al. for a TMT condition of MA957 [5], which is much stronger than the AE alloy. The σ for constant load-stress tests is slightly higher than measured in the SRJ tests. This difference is likely due to the fact that accumulated strains in the constant load-stress case were higher, leading to larger dislocation densities and smaller cell sizes.

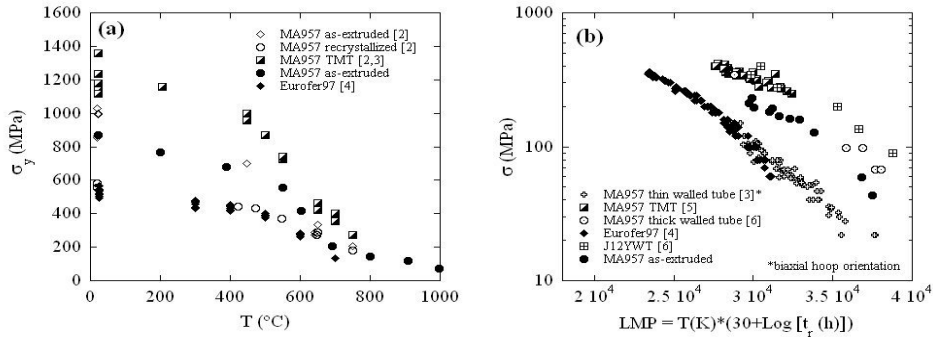


Figure 1 A comparison of: (a) $\sigma_y(T)$ for various alloys and alloy conditions; (b) creep rupture time LMP plots

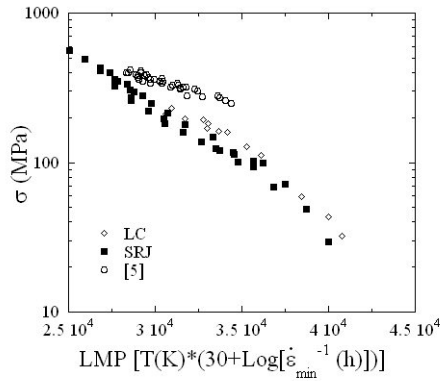


Figure 2 LMP for the inverse ϵ' for the AE MA957 SRJ tests, and CLS data for the AE and TMT MA957 [5].

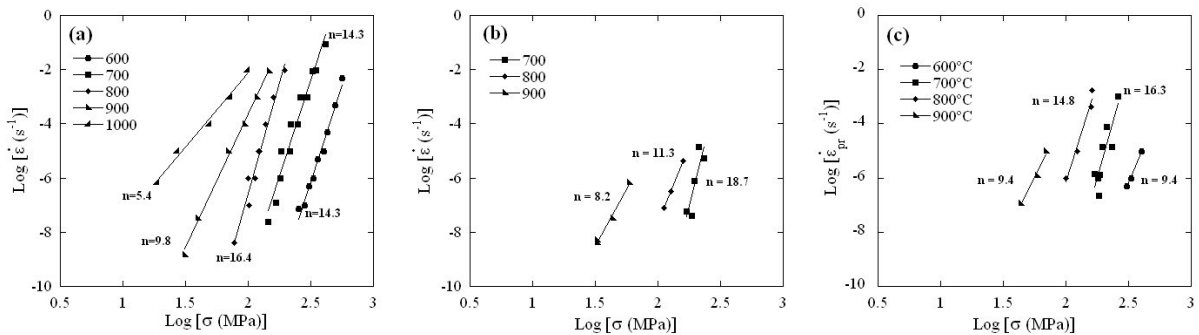


Figure 3 $\text{Log} \dot{\epsilon}'$ versus $\text{log} \sigma$ creep data for: (a) the SRJ tests; (b) the CLS tests; and, (c) the primary creep rate ($\dot{\epsilon}'_{pr}$) for CLS tests.

Figure 3a and b show plots of $\text{log} \dot{\epsilon}'$ versus $\text{log} \sigma$ data for the SRJ (3a) and constant load-stress (CLS) tests (3b) for the AE MA957, respectively. Figure 3c shows the corresponding primary average creep rates up to 0.5% from the CLS tests. The stress exponents (n) found by fitting the data to a standard

Norton power law creep model ($\dot{\epsilon}' \propto \sigma^n$) are shown in the plots. The fitted n range from 14.3 to 16.4 for the SRJ data from 600 to 800°C shown in Figure 3a, and decrease to 9.8 and 5.4 at 900 and 100°C, respectively. The n for the CLS test data shown in Figure 3b are lower, but both the data and stress ranges are both more limited in this case. The corresponding n values for the primary creep rates are higher and closer to those observed in the SRJ tests.

As commonly observed for dispersion strengthened alloys the creep behavior of MA957 is consistent with the existence of a threshold stress $\sigma_{tr}(T)$, below which creep ceases [7]. Thus $\dot{\epsilon}'$ can be better represented by

$$\dot{\epsilon}' = A \exp(-Q_{cr}/RT) \{[\sigma - \sigma_{tr}(T)]\}^n \quad (1)$$

The $\sigma_{tr}(T)$ were estimated by fitting Equation 1 to both the TMT MA957 literature data [5] and our measurements for AE condition. Typical n are ≈ 5 and Q_{cr} is the activation energy for creep which is expected to be close to the activation energy for self diffusion. Unconstrained fits resulted in somewhat higher n and Q_{cr} than anticipated by the threshold stress model. Thus to estimate σ_{tr} , which only weakly depends of n and Q_{cr} , these parameters were fixed at $n = 7$, at the high end of a physically plausible range and restricted to nominal self diffusion values of 250 to 300 kJ/mole. The fitted σ_{tr} for the AE condition are about 40 to 50% of σ_y from 600 to 800°C, decreasing to $\approx 18\%$ at 900°C and approaching 0% at 1000°C and are shown in Figure 4. The exact $\sigma_y(T)$ for the TMT MA957 is not know, but the σ_{tr}/σ_y ratio is believed to be as high, or even higher, in this case.

The physical basis for the high σ_{tr} is that the NF result in a minimum stress for dislocation climb and glide. We only briefly note that the most successful σ_{tr} creep model was proposed by Artz and co-workers [7], based on the hypothesis that the underlying mechanism is detachment of dislocations from attractive obstacles. Understanding the physical basis for $\sigma_{tr}(T)$ and its relation to the alloy microstructure, is key to optimizing the creep strength of NFA.

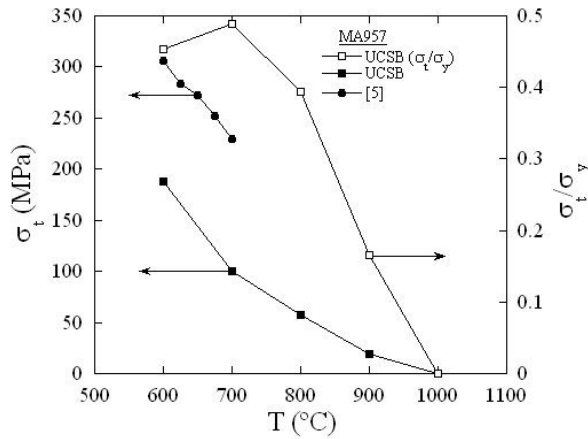


Figure 4 The $\sigma_{tr}(T)$ and σ_{tr}/σ_y for the TMT and AE MA957.

Figure 5 plots the primary creep (ϵ_{pr}) and creep rupture (ϵ_r) strains as a function of σ from 600 to 900°C for the constant load-stress tests. In both cases these strains tend to decrease with decreasing stress and increasing temperature.

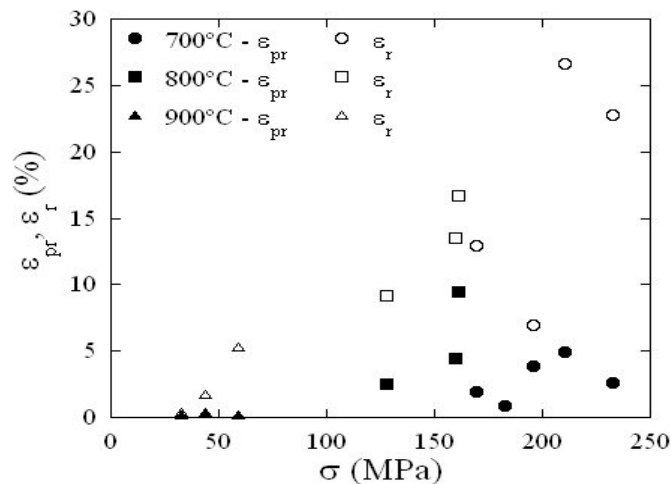


Figure 5 Primary and creep rupture strain data for CLS tests.

Figure 6 shows stress versus temperature plots for the 1000 h creep rupture time for TMT [5] and AE MA957. As well as the hoop stress for biaxial tests of extruded MA957 tubing [3] based on LMP fits. The TMT condition is about twice as strong as the AE MA957, which is about twice as strong as the tubing.

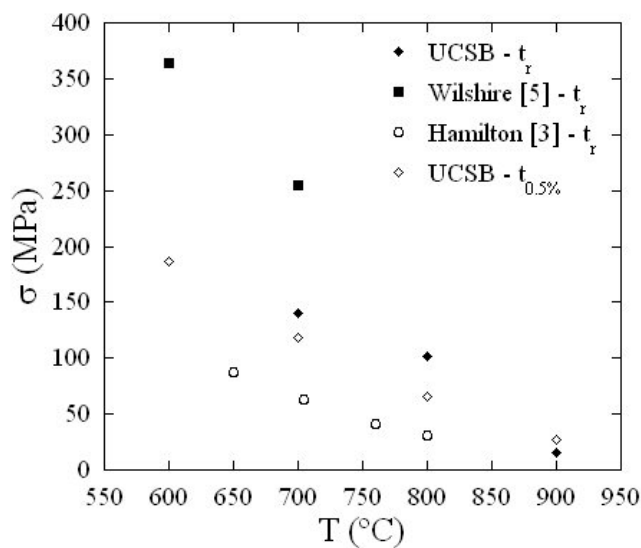


Figure 6 Predicted σ versus T plots for the 1000 h creep rupture and 0.5% primary strain times for various MA957 conditions and test orientations.

Summary and Future Work

The static and viscoplastic constitutive properties of AE MA957 were measured over a wide range of σ and T. Comparison of this data with that found in the literature shows that the strength of MA957 is generally higher than for TMS, but varies considerably, depending on the post-extrusion TMT and loading orientation relative to the extrusion direction. The creep data was fit the threshold stress model which shows that was $\sigma_{tr} > 0.4 \sigma_y$ up to 800°C. Testing and data analysis are continuing.

Acknowledgment

This research was partially funded by a DOE NERI Grant DE-FC07-05ID14663.

References

- [1] G.R. Odette, M.J. Alinger, and B.D. Wirth "Recent Developments in Irradiation Resistant Steels," Annual Reviews of Materials Research (to be published) (2008).
- [2] A. Alamo, V. Lambard, X. Averty, and M.H. Mathon, J. Nucl. Mater. 329-333 (2004) 333-337.
- [3] M.L. Hamilton, D.S. Gelles, R.J. Lobsinger, G.D. Johnson, W.F. Brown, M.M Paxton, R.J. Puigh, C.R. Eiholzer, C. Martinez, and M.A. Blotter, "Fabrication Technological Development of the Oxide Dispersion Strengthened Alloy MA957 for Fast Reactor Applications," PNL-13168, Pacific Northwest National Laboratory, Richland, WA (2000).
- [4] M. Rieth, M. Schirra, A. Falkenstein, P. Graf, S. Heger, H. Kempe, R. Lindau, and H. Zimmermann, "Eurofer97: Tensile, Charpy, Creep, and Structural Tests," FZKA6911, Forschungszentrum Karlsruhe (2003).
- [5] B. Wilshire and T.D. Lieu, Materials Science and Engineering A 386 (2004) 81-90.
- [6] D.T. Hoelzer, private communication.
- [7] E. Arzt and D.S. Wilkinson, Acta Metall. 34 (1986) 1893-1898.